

FLEXURAL CAPACITY CALCULATION OF RC BEAMS STRENGTHENED WITH PRESTRESSED CFRP SHEETS

Nguyen Dang Dai Nam¹, Ho Manh Hung^{1*}, Doan Cong Chanh^{1,2}, Phan Hoang Nam¹,
Nguyen Minh Hai¹, Gianluca Quinci³

¹The University of Danang - University of Science and Technology, Danang, Vietnam

²School of Engineering, Tra Vinh University, Tra Vinh, Vietnam

³Roma Tre University, Rome, Italy

*Corresponding author: hmhung@dut.udn.vn

(Received: September 08, 2024; Revised: October 09, 2024; Accepted: October 15, 2024)

DOI: 10.31130/ud-jst.2024.522E

Abstract - This paper investigates flexural behavior and analytical approach for predicting the load and deflection at critical performance points of reinforced concrete (RC) beams strengthened with prestressed carbon fiber-reinforced polymer (CFRP) sheets. A finite element model is developed to simulate the interaction between the RC beam and the CFRP sheets, capturing key aspects such as failure modes, ultimate load, and mechanical behavior across the three phases of failure. The analysis reveals that increasing the prestress level significantly enhances the performance, delaying the initiation of cracking, steel yielding, and increasing the ultimate load capacity. Two distinct failure modes are identified, i.e., concrete crushing in the compressive zone and composite plate peeling. An analytical approach is then proposed to estimate the load corresponding to initial cracking, steel yielding, and ultimate failure. Comparison between the experimental, numerical and analytical results shows that the proposed method accurately predicts the flexural capacity of RC beams strengthened with prestressed CFRP sheets.

Key words – Prestressed; CFRP sheets; FEM; analytical approach; flexural performance

1. Introduction

Over time, structures gradually exhibit signs of aging, leading to a decrease in their load-bearing capacity. Moreover, factors such as external environmental impacts and working under overload conditions further accelerate the degradation in the quality of structures [1]. Especially in reinforced concrete (RC) structures, the most common type of structure today, which is highly susceptible to environmental effects such as corrosion and abrasion due to erosion in coastal and river areas. Numerous strengthening methods for weakened positions have been proposed. Over the past decade, the use of external strengthening materials, such as steel plates, concrete, high-performance concrete, ultra-high-performance concrete, and fiber-reinforced polymer (FRP) composites, has become widespread. Among these, FRP stands out for its advantages, continuously affirming its superior properties, such as lightweight, high tensile strength, and corrosion resistance, and it is increasingly being applied [2].

The versatility and adaptability of FRP materials are key advantages. Different fiber types offer specific properties suited for various applications. Aramid fiber reinforced polymer (AFRP) provides high elongation, glass fiber reinforced polymer (GFRP) is a cost-effective option with good thermal resistance, carbon fiber

reinforced polymer (CFRP) delivers exceptional tensile strength and stress resistance, while basalt fiber reinforced polymer (BFRP) offers stable properties. With this range of FRP options, numerous studies have demonstrated their benefits in enhancing load-bearing capacity, delaying crack initiation, ensuring durability in harsh environments, and providing economic efficiency [3, 4].

However, a significant issue is the bonding process, where flexible FRP sheets, typically supplied in rolls, must be carefully applied to weakened structural areas. This process demands technical expertise, precision, and advanced construction methods. Poor execution or design can compromise FRP performance, particularly due to stress relaxation, which diminishes the effectiveness of the sheets during initial loading. To address this, prestressed FRP sheets are tensioned before bonding to the structure, providing a more efficient solution [5-7], though this method is still influenced by several factors.

Recent global research has focused on this issue. A series of experimental studies have evaluated the behavior of RC beams strengthened with prestressed FRP sheets to assess the impacts of various influencing factors. Notable examples include the effect of anchorage systems on prestressed FRP-strengthened RC beams [8-10], or the efficiency of different prestressed FRP materials, such as high-modulus CFRP (HM-CFRP), high-strength CFRP (HS-CFRP), and composite basalt and steel fibers (SW-BFRP) [11-13]. Additionally, the level of prestress applied to the FRP sheets is also a key focus. A variety of factors have been identified as having a significant influence on the effectiveness of prestressed FRP strengthening. On the other hand, aside from costly, time-consuming experimental studies that struggle to consider a wide range of reinforcement scenarios, numerical methods have also been applied and show great potential. Numerical studies are increasingly being improved, providing high accuracy and addressing challenges in numerical modeling. For example, Hu et al [14] solved the FRP-concrete interface problem using a cohesive model, while another study by Hawileh et al [15] used a spring element method to model this bond. Obidat et al [16] compared these methods with cohesive element methods to assess the pros and cons of different models. However, these studies remain fragmented and lack comprehensiveness as they primarily

simulate specific scenarios, without fully reflecting the impact of various design parameters on the flexural performance of prestressed FRP-strengthened structures.

This study aims to explore the flexural behavior of RC beams strengthened with prestressed CFRP sheets using numerical methods. A FEM is developed and validated, with a focus on the interaction between the CFRP and the concrete beam, to assess the mechanical behavior, flexural performance, and crack development in beams strengthened with both prestressed and non-prestressed CFRP sheets. Based on the analysis, critical points in the performance of the strengthened beams are identified, and an analytical approach is proposed to calculate the load and deflection of RC beams reinforced with prestressed CFRP sheets.

2. Numerical modeling

2.1. Description of case study

Three RC beam specimens presented in the previous experimental study of the authors were selected as the validation for the numerical analysis [17, 18]. The dimensions of the beams are detailed in Figure 1. Among these beams, one is an RC beam without prestressing, serving as a reference beam. The second beam is reinforced with a CFRP sheet but without prestressing (RC-CFRP-PR0), while the remaining beam is reinforced with a CFRP sheet prestressed to 500 MPa.

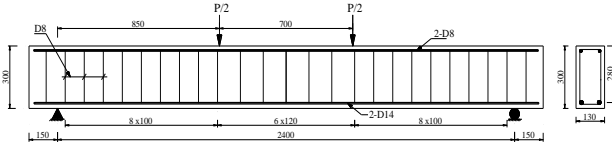


Figure 1. The parameters of RC beams

The compressive strength of the concrete was determined from standard specimens with dimensions of 150x150x150 mm, cured for 28 days with the average compressive strength for a set of 5 specimens was 35 MPa. The main tensile reinforcement consisted of steel bars with a diameter of 14 mm (D14), while the compressive reinforcement had a diameter of 8 mm. The yield strength and ultimate tensile strength of the D14 steel bars were determined from tensile testing, at 500 MPa and 720 MPa, respectively.

The CFRP sheets of the Sika CarboDur S1012 had a width of 100 mm and a thickness of 1.2 mm. The tensile strength and elastic modulus of the CFRP sheets were 3400 MPa and 165 GPa, respectively. The Sikadur-30 epoxy resin was used to bond the CFRP sheets to the concrete surface. The tensile strength of the Sikadur-30 adhesive after 7 days was measured at 3.5 MPa. A load of 60 kN was applied to the CFRP sheet in the experimental specimen, corresponding to approximately 15% of the tensile strength of the CFRP sheet.

The beam specimens were tested using a four-point bending setup with gradually increasing loads until failure. The flexural behavior was evaluated at three key points: (i) flexural cracking, (ii) reinforcement yielding, and (iii) ultimate failure.

2.2. FEM development

A three-dimensional finite element model is introduced

to simulate the flexural behavior of RC beams reinforced with FRP sheets using ABAQUS software [18, 19]. The model is set up with input parameters corresponding to those used in the previously mentioned experiment. The general model is illustrated in Figure 2. Concrete is assigned using solid elements capable of three-dimensional deformation, truss elements are used for the steel reinforcing bars deforming along their axis, and shell elements are assigned to the CFRP sheets with in-plane deformation capability.

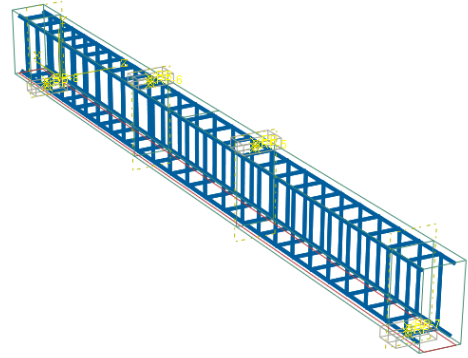
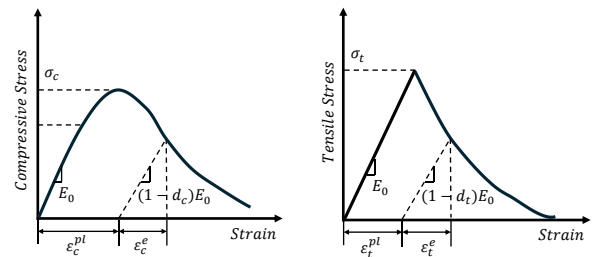
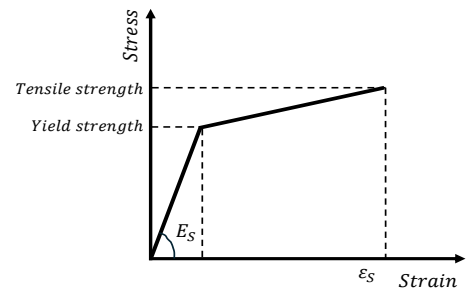


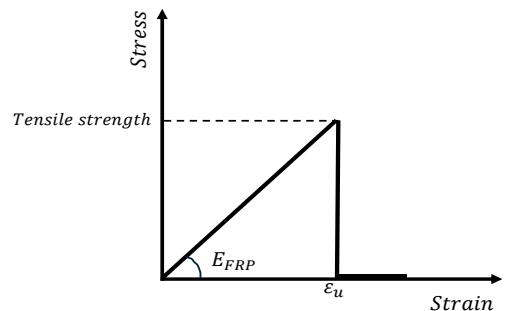
Figure 2. FEM model with the presence of reinforcements, concrete beam, and CFRP sheet



(a) Concrete model



(b) Steel model



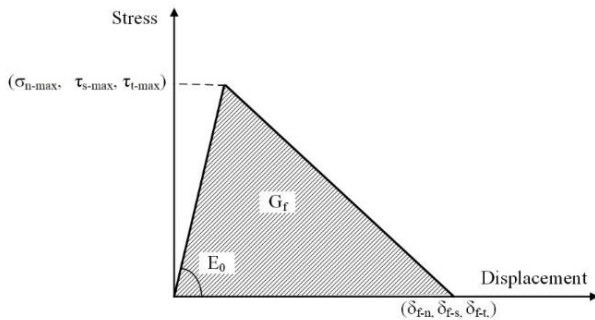
(c) FRP model

Figure 3. Material models

Table 1. Material parameters used in the FEM model

Concrete				
Compressive strength (MPa)	Tensile strength (MPa)	Young modulus (MPa)	Poisson ratio	Density (kg/m ³)
35	2	30000	0.15	2450
Dilation angle	Eccentricity	Equibiaxial to uniaxial initial yield ratio	Tensile to compress meridian slope K	Viscosity
35	0.1	1.16	0.667	0.00005
Steel				
Young modulus (MPa)	Poisson ratio	Yield strength (MPa)	Tensile strength (MPa)	
200000	0.3	500	720	
CFRP				
Young modulus (MPa)		Tensile strength (MPa)		
165000		3400		

Regarding materials, the concrete damaged plasticity (CDP) model [20] is employed to simulate the failure of concrete in both tension and compression regions (Figure 3(a)). For steel, the bilinear model is used, with parameters such as yield strength, ultimate strength, and the slope of the yield plateau obtained from tensile testing of steel (Figure 3(b)). Due to the characteristics of CFRP material, a simple material model is described through a linear relationship, where, upon reaching the tensile failure strength, the CFRP breaks, and the stress drops to zero (Figure 3(c)). A summary of material parameters is shown in Table 1.

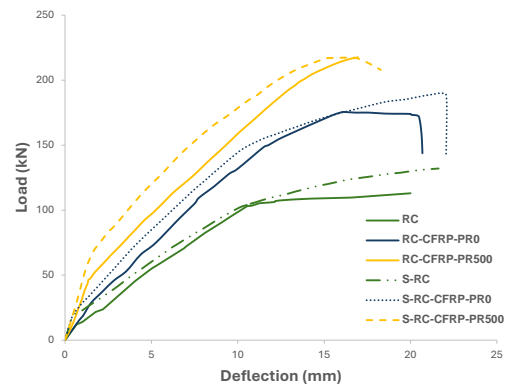
**Figure 4.** Bond-displacement relationship in the cohesive model between concrete and FRP sheet

The initial stress method is used, applying a prestress directly to the CFRP sheet [19]. The steel-concrete bond is modeled using a hard contact that has been proven to be highly reliable in previous studies [21]. A cohesive behavior model is introduced to describe the complexity of the concrete-CFRP bond interaction [16, 22, 23]. Specifically, the cohesive behavior model [14, 24] allows for the definition of the bond through initial stiffness, normal and shear bond strengths, with the characteristics determined based on the technical parameters of the Sikadur-30 epoxy resin. The initial stiffness is set according to the elastic modulus of the epoxy adhesive, at 4.5 GPa, while the bond strengths in the normal and shear directions are 3.5 MPa and 7.0 MPa, respectively.

With the simple geometric features of the beam components, the automatic meshing function was employed. The mesh edge lengths were set to 40 mm, 25 mm, and 20 mm, respectively.

Table 2. Comparison between experiment and simulation results

Specimens	Flexural crack		Reinforcement yielding		Ultimate failure	
	P_{1Exp} (kN)	P_{1Sim} (kN)	P_{2Exp} (kN)	P_{2Sim} (kN)	P_{3Exp} (kN)	P_{3Sim} (kN)
RC	12.3	15.3	103.5	104.5	109.6	116.1
Exp/Ana	0.80		0.99		0.94	
RC-CFRP-PR0	15.2	18.0	150.0	151.6	175.6	184.7
Exp/Ana	0.84		0.99		0.95	
RC-CFRP-PR500	46.3	53.4	198.8	208.2	217.7	217.4
Exp/Ana	0.87		0.95		1.00	

**Figure 5.** Comparison of the load-deflection relationship between experiment and simulation

The numerical analysis results are presented in Figure 5 and summarized in Table 2 together with the previous experimental results. It is noticed that the simulated beam models were labeled with the prefix "S", representing simulation. In general, the simulation results show a high degree of agreement with the experimental results. Firstly, for the point at which the first flexural crack appears, the ratio between experimental and simulated values ranges from 0.8 to 0.87. Next, the ratio between the experimental and simulated values at the yield point of the reinforcing steel ranges from 0.95 to 0.99. Moreover, for the ultimate failure point of the beam, this ratio fluctuates between 0.94 and 1.0. These findings demonstrate that the model performs well in simulating post-crack behavior, closely capturing the behavior and load-bearing capacity of CFRP-reinforced beams in the experiment.

Specifically, for the beam model S-RC-CFRP-PR500, the correlation is very high at all three critical points. At the flexural crack initiation point P_1 , the experimental result is 46.3 kN, while the simulated result is 53.4 kN ($\approx 87\%$). At the yield point of the reinforcing steel P_2 , the experimental and simulation results are 198.8 kN and 208.2 kN, respectively ($\approx 95\%$). For the ultimate failure state P_3 or P_u , these results are 217.7 kN and 217.4 kN ($\approx 100\%$), respectively. This high level of correlation shows that, after the initial crack formation stage, the simulation results almost perfectly align with the experimental results.

3. Analytical model development

3.1. Analysis of performance phrases of beams based on numerical results

The behavior of RC beams reinforced with prestressed FRP sheets can be divided into three stages: (i) the elastic stage, (ii) the crack development stage, and (iii) the elastic-plastic stage, as illustrated in Figure 6.

In the elastic stage, the concrete is uncracked, and the deflection increases linearly with the load. The load P_1 corresponds to the point at which flexural cracks first appear in the concrete. The stiffness in this stage is denoted as α_1 . In the crack propagation stage, the cracks in the concrete begin to widen and develop. The tensile reinforcement remains in the elastic region until it reaches the load P_2 , which corresponds to the yield stress of the steel at the maximum bending section. The stiffness in this stage is denoted as α_2 . In the third stage, the concrete is fully cracked, the tensile reinforcement yields, and the failure region progresses toward the ultimate failure, with the corresponding load referred to as the ultimate load P_3 or P_u .

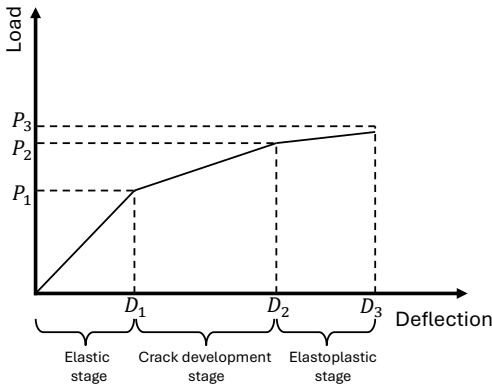


Figure 6. Different stages of the mechanical behavior of the beam

3.2. Analytical model development

A theoretical analytical model based on equilibrium equations is developed in this section to describe the behavior of reinforced concrete beams (RC beams) under bending, strengthened with prestressed FRP sheets. The model is based on cross-sectional parameters and material properties. On this basis, the stresses at the fibers of the cross-sectional area at different stages are calculated through the mechanical behavior of the beam.

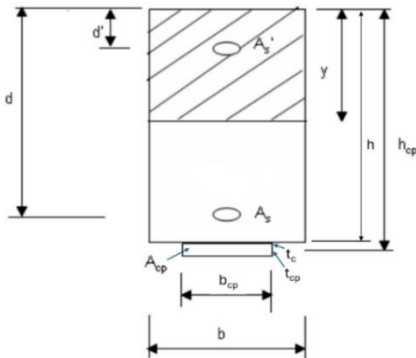


Figure 7. Cross-section of the concrete beam reinforced with CFRP sheets

Stage 1: In this stage, the concrete is uncracked. All

materials are homogeneous within a concrete cross-section. The position of the neutral axis can be calculated by transforming the forces within the homogeneous section (Figure 7),

$$y = \frac{[n(d'A_s' + dA_s) + n_{cp}A_{cp}(h + t_c + t_{cp}/2) + bh]}{n(A_s' + A_s) + n_{cp}A_{cp} + bh} \quad (1)$$

Considering the effects of reinforcement and FRP sheets, the moment of inertia of the equivalent section can be calculated as

$$I = \frac{by^3}{3} + \frac{b(h-y)^3}{3} + nA_s(d-y)^2 + n_{cp}A_{cp}(h_{cp}-y)^2 \quad (2)$$

In the elastic stage, the load-deflection relationship is governed by the equation

$$P_1 = \alpha_1 D_1 \quad (3)$$

$$\text{where } \alpha_1 = \frac{E_b I_{nf}}{c} \text{ and } c = a \frac{3L^2 - 4a^2}{48} \quad (4)$$

with a being the distance from the support to the load point and L is the span length.

When the beam is subjected to bending under the load and the prestressing force of the FRP sheet, the stress at the top and bottom fibers of the section is given by

$$\sigma(y) = -\frac{F_{cp}}{S} \pm \frac{F_{cp}e_0y}{I} \mp \frac{My}{I} \quad (5)$$

where e_0 is the distance between the neutral axis and the FRP sheet, F_{cp} is the prestressing force of the FRP sheet, and S is the section modulus of the concrete, with compression being denoted as negative (-) and tension as positive (+). When flexural cracks appear, the tensile stress at the bottom fiber of the section reaches the tensile strength limit of the concrete. From equation (5), we have

$$f'_t = -\frac{F_{cp}}{bh} - \frac{F_{cp}(h_{cp}-y)(h-y)}{I} + \frac{P_1 a(h-y)}{2I} \quad (6)$$

After a simple transformation, the load P_1 , corresponding to the initial cracks in the concrete, can be evaluated by the equation,

$$P_1 = 2(f'_t + \frac{F_{cp}}{bh}) \frac{I}{a(h-y)} + 2F_{cp} \frac{(h_{cp}-y)}{a} \quad (7)$$

where f'_t is the tensile strength limit of the concrete.

Stage 2: In this stage, the calculation of the neutral axis position is performed by the static equilibrium of the homogeneous section, neglecting the influence of the tensile concrete. The position of the neutral axis is the solution to the equation

$$0 = \frac{by^2}{2} + nA_s'(y-d') + nA_s(d-y) - n_{cp}A_{cp}(h_{cp}-y). \quad (8)$$

The moment of inertia of the homogeneous section can be calculated using the general formula

$$I = \frac{by^3}{3} + nA_s'(y-d')^2 + nA_s(d-y)^2 - n_{cp}A_{cp}(h_{cp}-y)^2. \quad (9)$$

The load-deflection relationship is determined by

$$\Delta P = \alpha_2 \Delta D, \quad (10)$$

$$\text{where } a_2 = \frac{E_b I_f}{c} \text{ and } c = a \frac{(3L^2 - 4a^2)}{48} \quad (11)$$

It is assumed that the moment of inertia of the section does not change along the beam. However, under bending loads, the section remains uncracked in the region $x < x_{CR}$ (the position at the cracking moment M_{CR}) and cracked in the region $x > x_{CR}$. Considering the uncracked (with I_{nf}) and cracked regions (with I_f), a new expression for deflection can be obtained using equation (12),

$$D = 2 \left[\frac{1}{EI_{nf}} \int_0^{x_{CR}} \frac{x}{2} M(x) dx \right] + \frac{1}{EI_f} \int_{x_{CR}}^{L-x_{CR}} \frac{x}{2} M(x) dx \quad (12)$$

For four-point bending, the bending moment $M(x)$ is calculated as

$$M(x) = \frac{Px}{2} \quad (13)$$

The concrete remains uncracked when $0 < x < x_{CR}$ and $x_{CR} = 2 \frac{M_{CR}}{P}$

Then, equation (12) becomes

$$D = \frac{Px_{CR}^3}{6EI_{nf}} + \frac{P}{48EI_f} [a(3L^2 - 4a^2) - 8x_{CR}^3] \quad (14)$$

The load P_2 corresponding to the yielding of the tensile reinforcement, and the corresponding deflection D_2 are calculated according to equation (3.14). In general, the stress at the bottom fiber of the homogeneous concrete section can be relatively calculated as

$$\sigma(y) = -\frac{F_{cp}}{S} - \frac{F_{cp}e_0y}{I} + \frac{My}{I} \quad (15)$$

For steel in the tensile region, $y = -(d - y)$, equation (15) can be rewritten as

$$\sigma(-(d - y)) = n \left(-\frac{F_{cp}}{S} - \frac{F_{cp}e_0(d - y)}{I} + \frac{M(d - y)}{I} \right) \quad (16)$$

When the steel yields, the stress in the steel equals the yield strength f_{yk} . From equation (16), the load P_2 , corresponding to the yielding of the tensile steel, can be evaluated by the equation

$$f_{yk} = -\frac{nF_{cp}}{bh} - \frac{F_{cp}(h_{cp} - y)(d - y)n}{I} - \frac{P_2 a(d - y)n}{2I} \quad (17)$$

Therefore

$$P_2 = -\frac{2If_{yk}}{na(d - y)} + \frac{F_{cp}2I}{abh(d - y)} - \frac{2F_{cp}(h_{cp} - y)}{a} \quad (18)$$

The deflection corresponding to P_2 is determined from ΔF_2 and F_2

$$D_2 = D_1 + \Delta D_2$$

Stage 3: In this stage, the tensile reinforcement (A_s)

operates in the plastic region and strain-hardening region; hence, a new modular ratio n' is applied. The value of n' is calculated as the ratio between the modulus of elasticity in the strain-hardening region of the steel and the elastic modulus of the concrete. This ratio is significantly smaller than in the elastic stage; therefore, the contribution of the tensile reinforcement to the stiffness of the section is significantly reduced in stage 3.

The position of the neutral axis is calculated as in stage 2, considering the modular ratio n' for the tensile reinforcement (assuming that the strain-hardening region is linear). As a result, there is a solution to the equation

$$0 = \frac{by^2}{2} + nA'_s(y - d') + n'A_s(d - y) - n_{cp}A_{cp}(h_{cp} - y) \quad (19)$$

The moment of inertia of the homogeneous section in stage 3 is given by

$$I = \frac{by^3}{3} + nA'_s(y - d')^2 + n'A_s(d - y)^2 - n_{cp}A_{cp}(h_{cp} - y)^2 \quad (20)$$

In stage 3, the load-deflection relationship is governed by the equation

$$\Delta P = \alpha_3 \Delta D, \quad (21)$$

where $a_3 = \frac{E_b I_f}{c}$ and $c = a \frac{3L^2 - 4a^2}{48}$. (22)

In a bending structure, the stress gradient in the FRP sheet generates shear stress on the interface between the FRP sheet and the concrete (Figure 8). Between two sections separated by a distance dx , the generated shear stress is calculated as

$$\tau(x) = \frac{F(x + dx) - F(x)}{b_{cp} dx} \quad (23)$$

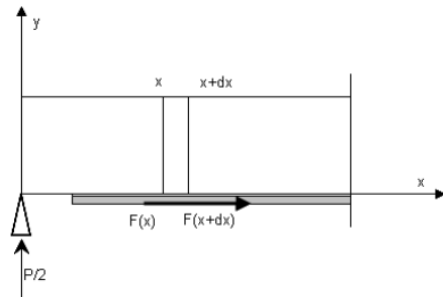


Figure 8. Shear stress on the interface of the FRP sheet and concrete

The stress in the FRP layer depends on the bending moment of the section, therefore

$$\sigma_{cp}(x) = \sigma(x, y) = \sigma(h_{cp} - y_f) = n_{cp} \frac{M(x)(h_{cp} - y_f)}{I_f} \quad (24)$$

The tensile force is calculated as

$$F(x) = \sigma_{cp}(x) b_{cp} t_{cp}. \quad (25)$$

Therefore, the shear stress at x is calculated as

$$\tau(x) = \frac{M(x + dx) - M(x) n_{cp}(h_{cp} - y_f)}{b_{cp} dx} b_{cp} t_{cp} \quad (26)$$

After simplification, equation (26) becomes

$$\tau(x) = \frac{dM(x)}{dx} \frac{n_{cp} t_{cp} (h_{cp} - y_f)}{I_f} \quad (27)$$

In a four-point bending, the deformation due to shear is calculated as

$$\tau(x) = \frac{P}{2} \frac{n_{cp} t_{cp} (h_{cp} - y_f)}{I_f} \quad (28)$$

Failure begins when the shear stress in the concrete reaches the limit, specifically when $\tau(x) = \tau_u$.

The load in stage 3 is determined by the formula

$$P_3 = - \frac{2I_f \tau_u}{n_{cp} t_{cp} (h_{cp} - y_f)} \quad (29)$$

The results obtained from the analytical model for the RC-CFRP-PR500 beam specimen are presented in Table 3. The established equation for calculating the flexural capacity of the RC beam strengthened with prestressed CFRP shows a high level of accuracy compared to the experimental results at two critical points which is the most significant for an RC beam strengthened, the flexural crack and the ultimate failure points. For the load at the concrete cracking point due to flexure, the calculated value differs by 6.37% from the experiment values. The difference at the ultimate failure point between the experimental and calculated values is almost negligible, below 0.2%. From this, the prediction of the load at critical points of the RC beam strengthened using prestressed CFRP through the formula calculation model is entirely feasible and even yields promising results.

Table 3. Comparison between experiment and analytical model results

Specimens	Flexural crack		Ultimate failure	
	P_{1Exp} (kN)	P_{1Cal} (kN)	P_{3Exp} (kN)	P_{3Cal} (kN)
RC-CFRP-PR500	46.3	43.35	217.72	218.13
Exp/Ana	6.37%		0.18%	

3.3. Comparison of FEM and analytical model

Both the analytical and numerical models produced highly accurate results when compared to the experimental data. While minor discrepancies remain, they are likely due to incomplete input data and unaccounted factors during the experimental process. A comparison between the analytical and numerical models at key points, specifically the flexural crack point and the ultimate failure point, is presented in Table 4.

It is evident that not only when compared to the experimental values, but also when compared to each other, both the analytical and numerical models demonstrate closely correlated results. In stage 1, the analytical model provides a better estimation of the load at the point of crack initiation, with higher accuracy (1.06) compared to the numerical model (0.87). On the other hand, in stage 3, at the point of the failure of the beam, both models exhibit almost no discrepancy in the load results (≈ 1) compared to the experimental data. This further confirms the reliability and accuracy of the numerical approach in general, as well as the two models developed

in this study to investigate the flexural performance of RC beams strengthened with prestressed CFRP sheets.

Table 4. Comparison among numerical model, analytical model and experiment values

Stage	Parameter	RC-CFRP-PR500	
1	$P_1(Anl)$ (kN)	43.35	
	$P_1(Num)$ (kN)	46.3	
	$P_1(Anl)/P_1(Num)$	0.94	
	$P_{1Exp} / P_1(Anl/Num)$	1.06	0.87
3	$P_3(Anl)$ (kN)	218.13	
	$P_3(Num)$ (kN)	217.4	
	$P_3(Anl)/P_3(Num)$	1.003	
	$P_{3Exp} / P_3(Anl/Num)$	≈ 1.00	≈ 1.00

4. Conclusions

This paper investigated the flexural performance of RC beams strengthened with prestressed CFRP sheets through a numerical modeling approach. Then, a formula for the flexural capacity calculation was presented for RC beams strengthened with prestressed CFRP sheets. The results lead to the following conclusions:

i) The comparison of the load-deflection results between the finite element model and the experimental results shows that the numerical model developed in this study provides reliable results in simulating the flexural behavior of reinforced concrete (RC) beams strengthened with prestressed CFRP sheets.

ii) Based on the load-deflection relationship, the use of prestressed CFRP sheets in the flexural strengthening of RC beams has proven highly effective in delaying the appearance of cracks, steel yielding, and increasing the ultimate load capacity of the strengthened beams.

iii) Based on the analysis results, the study also presented the performance stages of RC beams strengthened with prestressed CFRP sheets, including the elastic stage, crack development stage, and elastoplastic stage. Based on these working stages, a theoretical expression was developed for calculating the load and deflection of the strengthened beams at critical points. The comparison between the theoretical formula and the finite element model shows that the formula can calculate the load and deflection of RC beams strengthened with prestressed CFRP sheets with high accuracy.

REFERENCES

- [1] M. Sanchez-Silva, G.-A. Klutke, and D. V. Rosowsky, "Life-cycle performance of structures subject to multiple deterioration mechanisms", *Structural Safety*, vol. 33, no. 3, pp. 206-217, 2011.
- [2] Y. Zhu, Y. Zhang, H. H. Hussein, and G. Chen, "Flexural strengthening of reinforced concrete beams or slabs using ultra-high performance concrete (UHPC): A state of the art review", *Engineering Structures*, vol. 205, p. 110035, 2020.
- [3] M. N. Danraka, H. M. Mahmood, O.-k. J. Oluwatosin, and P. Student, "Strengthening of reinforced concrete beams using FRP technique: a review", *International Journal of Engineering Science*, vol. 7, no. 6, p. 13199, 2017.
- [4] J. D. Ortiz, S. S. Khedmatgozar Dolati, P. Malla, A. Nanni, and A. Mehrabi, "FRP-reinforced/strengthened concrete: State-of-the-art

- review on durability and mechanical effects”, *Materials*, vol. 16, no. 5, p. 1990, 2023.
- [5] R. Wight, R. El-Hacha, and M. Erki, "Prestressed and non-prestressed CFRP sheet strengthening: damaged continuous reinforced concrete beams”, *International Journal of Materials and Product Technology*, vol. 19, no. 1-2, pp. 96-107, 2003.
- [6] P. Yu, P. F. Silva, and A. Nanni, "Flexural performance of RC beams strengthened with prestressed CFRP sheets”, *Center for Infrastructure and Engineering Studies Department of Civil, Architectural, and Environmental Engineering University of Missouri-Rolla Rolla, MO*, pp. 65409-0030, 2003.
- [7] H.-T. Wang, Q. Wu, C.-Y. Zhu, Y.-H. Mao, and C.-C. Guo, "An innovative prestressing system of prestressed carbon fiber sheets for strengthening RC beams under flexure”, *Construction and Building Materials*, vol. 411, p. 134409, 2024.
- [8] R. El-Hacha and M. Y. Aly, "Anchorage system to prestress FRP laminates for flexural strengthening of steel-concrete composite girders”, *Journal of Composites for Construction*, vol. 17, no. 3, pp. 324-335, 2013.
- [9] Y. J. Kim, R. G. Wight, and M. F. Green, "Flexural strengthening of RC beams with prestressed CFRP sheets: Development of nonmetallic anchor systems”, *Journal of Composites for Construction*, vol. 12, no. 1, pp. 35-43, 2008.
- [10] Y. Wang, Q. Jia, R. Surahman, and X. He, "Static and seismic strengthening of RC frame joints by using CFRP sheets with various anchoring methods”, *Journal of Building Engineering*, vol. 82, p. 108309, 2024.
- [11] N. Attari, S. Amziane, and M. Chemrouk, "Flexural strengthening of concrete beams using CFRP, GFRP and hybrid FRP sheets”, *Construction and Building Materials*, vol. 37, pp. 746-757, 2012.
- [12] Z. Chen *et al.*, "Evaluation of CFRP, GFRP and BFRP material systems for the strengthening of RC slabs”, *Journal of reinforced plastics and composites*, vol. 27, no. 12, pp. 1233-1243, 2008.
- [13] S. S. Choobor, R. A. Hawileh, A. Abu-Obeidah, and J. A. Abdalla, "Performance of hybrid carbon and basalt FRP sheets in strengthening concrete beams in flexure”, *Composite Structures*, vol. 227, p. 111337, 2019.
- [14] B. Hu, J.-g. Wang, and G.-q. Li, "Numerical simulation and strength models of FRP-wrapped reinforced concrete columns under eccentric loading”, *Construction and building materials*, vol. 25, no. 5, pp. 2751-2763, 2011.
- [15] R. A. Hawileh, "Nonlinear finite element modeling of RC beams strengthened with NSM FRP rods”, *Construction and Building Materials*, vol. 27, no. 1, pp. 461-471, 2012.
- [16] Y. T. Obaidat, S. Heyden, and O. Dahlblom, "The effect of CFRP and CFRP/concrete interface models when modelling retrofitted RC beams with FEM”, *Composite structures*, vol. 92, no. 6, pp. 1391-1398, 2010.
- [17] M. H. Nguyen, M. H. Ho, V. R. Tran, H. N. Phan, D. D. N. Nguyen, and P. N. Huynh, "Flexural performance of reinforced concrete beams strengthened with prestressed FRP sheets: Experiments and numerical investigations”, *Case Studies in Construction Materials*, vol. 21, 2024, doi: 10.1016/j.cscm.2024.e03475.
- [18] M. H. Ho, N. P. PHam, and H. N. Phan, "An experimental study on the flexural strengthening of reinforced concrete beams using prestressed CFRP plates”, *Journal of Science and Technology in Civil Engineering (JSTCE) – Hanoi University of Civil Engineering (HUCE)*, vol. 15, no. 7V, pp. 109-118, 2021.
- [19] Hibbitt, Karlsson, and Sorensen, *Abaqus/CAE User's Manual*. Hibbitt, Karlsson & Sorensen, Incorporated, 2002.
- [20] A. U. Manual, "Abaqus user manual”, *Abacus*, 2020.
- [21] H.-G. Kwak and F. C. Filippou, *Finite element analysis of reinforced concrete structures under monotonic loads*. Citeseer, 1990.
- [22] C. Yuan, W. Chen, T. M. Pham, H. Li, and H. Hao, "Finite element modelling of dynamic bonding behaviours between fibre reinforced polymer sheet and concrete”, *Construction and Building Materials*, vol. 255, p. 118939, 2020.
- [23] H. Niu and Z. Wu, "Effects of FRP-concrete interface bond properties on the performance of RC beams strengthened in flexure with externally bonded FRP sheets”, *Journal of materials in civil engineering*, vol. 18, no. 5, pp. 723-731, 2006.
- [24] P. Qiao and Y. Chen, "Cohesive fracture simulation and failure modes of FRP-concrete bonded interfaces”, *Theoretical and applied fracture mechanics*, vol. 49, no. 2, pp. 213-225, 2008.